TREE SPECIES RECOGNITION AT STANDS SCALE: VALIDITY TEST OF MULTI-TEXTURE EXTRACTED FROM MULTI-SEASONAL UAV-BASED IMAGERY

LIU, H. P.

School of Land and Tourism, Luoyang Normal University, Luoyang, Henan Province 471934, China
e-mail: gatestudy@163.com

(Received 6th Dec 2022; accepted 27th Feb 2023)

Abstract. In order to evaluate the effectiveness of multi-type texture features of images of four seasons in pure stand tree species recognition, this research applied 5-band RedEdge-MX sensor to collect remote sensing data of four seasons and extracted eight texture features, including mean, variance, homogeneity, contrast, dissimilarity, entropy, second moment and correlation, from 20 spectral bands. Maximum likelihood classification and random forest were adopted for the determination of the best window for texture extraction which resulted in the construction of optimal texture feature set in tree species recognition. Then, the performance of these texture feature sets along with their combinations in tree species recognition was analyzed. Experimental findings showed that the eight texture features of four seasonal data performed well in the recognition of pure stand tree species. Texture feature mean presented the highest performance (with overall accuracy of 88.8559%) and worst variance (84.8180%). The combination of eight texture features further improved the recognition accuracy of tree species (92.0599%) compared with single texture features. The recognition accuracy of tree species could be further improved by combining eight texture features with spectral band and digital surface model (92.7002%). Research showed that the application of multi-type texture features in typical seasons of spring, summer, autumn and winter fully captured the differences of various tree species in different bands and seasons, which could be applied to the effectively identify pure stand tree species in regular plots.
Keywords: *four-season RedEdge-MX data, regular pure stands, tree species recognition, eight texture types application, effectiveness evaluation*

Abbreviations:
CON: Contrast, COR: Correlation, DEM: Digital elevation model, DIS: Dissimilarity, DL: Deep learning, DSM: Digital surface model, ENT: Entropy, HOM: Homogeneity, KC: Kappa coefficient, MEA: Mean, MLC: Maximum likelihood classifier, OA: Overall accuracy, RF: Random forest, ROI: Region of Interest, RS: Remote sensing, SM: Second moment, SVM: Support vector machine, TS: Tree species, UAV: Unmanned aerial vehicle, VAR: Variance

Introduction

Tree species (TS) of regular pure stands are commonly grown in nursery bases, germplasm resource nursery and botanical gardens. Due to the special environment where these TS are located, they have great value in terms of application, scientific research and ornament. Therefore, managing these TS is of critical importance. Identification of TS through remote sensing (RS) methods in these types of plots can provide certain technical means to assess tree growth, monitor dynamic change and analyse planting structure, which is of great significance. Since TS distribution in these plots is more homogeneous than other environments (e.g. same environment, age and tree height), it is possible to accurately identify these TS via RS technology. Therefore, conducting active research on TS identification in these plots is also practically feasible.

Recently, the most representative satellite data used for TS identification using RS technology were high spatial resolution imagery such as IKONOS, QuickBird, and

WorldView-2/-3 (Immitzer et al., 2012; Pu and Landry, 2012; Wang et al., 2016; Ferreira et al., 2019; Yan et al., 2021). Application of these data demonstrated that the pixel size and spectral band number of an image substantially influenced the classification accuracy of TS and data with high spatial and/or spectral resolution increased discrimination accuracy in a certain range of area. Then, other data such as radar, digital elevation model (DEM) and digital surface model (DSM) were combined (Naidoo et al., 2012; Kamal et al., 2015; Åkerblom et al., 2017; Torabzadeh et al., 2019; Pu and Landry, 2020). These data with ground object height information, can be for applied in TS classification to improve the accuracy of identification. Currently, with the iteration of unmanned aerial vehicle (UAV) engineering, low-altitude airborne multispectral and hyperspectral data are extensively applied for TS identification (Wang et al., 2020; Zhang et al., 2020). Researchers have applied spectral bands, vegetation indices, texture layers and DSMs for the classification of TS based on the above-mentioned data (Wang et al., 2016; Åkerblom et al., 2017; Yu et al., 2017; Pu et al., 2018). They concluded that textures and DSMs were better compared to other image features for TS classification, and the combined of various data and a great number of features in RS data enhanced the accuracy of TS recognition (Cross et al., 2019; Apostol et al., 2020). They also proved that hyperspectral imagery had a better discrimination ability than multispectral imagery for TS identification (Richards and Jia, 2008; Zhang et al., 2016; Kureel et al., 2021). In addition, researchers have attempted to create refreshing features that were helpful in TS identification and enhanced the differentiated TS information in images from other perspectives (Zhou et al., 2011; Liu and An, 2020).

To determine imaging time period of RS data for TS identification, research works have generally applied only single period data, generally tree leafy season (summer) data, for TS classification (Li et al., 2015; Liu et al., 2015; Liu and An, 2019). Some subsequent studies have proved that TS recognition effect using summer images was not as effective as that adopting the data collected from the other three seasons (Pu et al., 2018; Liu, 2022). Application of a single period RS data failed to perceive image changes due to TS reflectance at different time periods, resulting in low recognition accuracy. More recently, some researchers have introduced multiple time series data for TS identification to enhance the reflection of phenological information on images (Dymond et al., 2002; Hamraz et al., 2019; Masemola et al., 2019, 2020; Shi et al., 2020). They found that the application of a series of multiple period data allowed more accurate TS identification than adopting single period data (Li et al., 2015; Han et al., 2019; Immitzer et al., 2019). However, TS have yet to be identified based on image texture features at several critical periods such as tree flowering and budding, leafy, leaf colour change and post deciduous leaf periods. The effectiveness of single-type textures as well as the combination of multi-type textures in these time node images in TS recognition remains unclear. Regarding the widespread application of low-altitude UAVs, data collection time could be flexibly determined and data on key time nodes on vegetation growth could be easily acquired, which was beneficial for solving this question.

For the application of TS identification classifiers, maximum likelihood classifier (MLC), support vector machine (SVM) and random forest (RF) have been extensively adopted (Li et al., 2015; Lin et al., 2015; Pu et al., 2018; Modzelewska et al., 2020). Currently, with the popularity of deep learning (DL) technology, some researchers apply this method to classify TS to improve classification accuracy (Kemal et al., 2019; Niu et al., 2019; Shi et al., 2019; Zhang et al., 2019; Zhong et al., 2019). Among these methods, MLC presented excellent performance (high speed and accuracy) in low-dimensional data

http://www.aloki.hu ● ISSN 1589 1623 (Print) ● ISSN1785 0037 (Online)
DOI: http://dx.doi.org/10.15666/aeer/2102_15151532

classification. However, Hughes phenomenon occurs in high-dimensional data classification, which is not conducive to judge which feature sets are more important (Ghosh and Joshi, 2014). SVM achieved high accuracy and was insensitive to feature dimension, but it was time-consuming (Ferreira et al., 2016). DL was also not sensitive to data dimension and achieved high accuracy, but it needed a long training time. When RF was used, it not only was insensitive to data dimension, but also had relatively less training time and very high recognition accuracy. In addition, it could rank feature importance. High-dimensional data have several features with rich ground object information. However, due to data dimensionality issues, MLC is inappropriate and other classifiers have to be applied. For low-dimensional data in which the number of classification features is relatively small, MLC can be the best choice; however, when the number of used classification features is comparatively large and less time is needed to process them, RF may be a better choice.

Literature review revealed that in research on TS identification, researchers have fully considered imagery type, imaging time, and spatial and spectral resolution as well as the application of multiple feature types and suitable classifiers. For RS data, texture features formed pixel clusters with relatively similar pixel values in images resulting in the generation of relatively homogeneous image regions. In the texture layer of the image, these homogeneous areas corresponded well with pure stand TS distribution. Theoretically, image texture features can better characterize the space distribution of various pure stand TS. During the four seasons of the year (tree flowering and budding, leafy, leaf colour change and post deciduous leaf periods), trees presented significantly different texture reflections in images. We think that texture features extracted from the images captured in the above four key time nodes could drive pure stand TS discrimination. In the current research, we applied low-altitude UAV to capture RedEdge-MX imagery in the above time nodes to extract eight types of texture features, i.e. mean (MEA), variance (VAR), homogeneity (HOM), contrast (CON), dissimilarity (DIS), entropy (ENT), second moment (SM) and correlation (COR). Then, we constructed single-type and combined/mixed texture feature sets and combined mixed texture feature set with DSM and spectral bands. Finally, we classified TS based on these feature sets using MLC and RF classifiers. The main purpose of this research was to evaluate the performance of eight texture feature types derived from UVA-based imagery of four seasons for pure stand TS identification to provide basic information for high-precision mapping of pure stand TS.

Materials and methods

Data acquisition and preprocessing

RedEdge-MX imagery

The research area (~2.2 ha) was located on the new campus of Luoyang Normal University in Luoyang, Henan Province, China (*Fig. 1*). The materials employed in this research were obtained by airborne (JOUAV CW-15, Produced by China Chengdu Zongheng Co., Ltd) RedEdge-MX sensor (produced in Micasense Company of American) and the data obtained for each season had five spectral bands of blue, green, red, red edge and near infrared and one DSM (Agarwal et al., 2021). *Table 1* summarizes the detailed parameters of band setting, wavelength range and spatial resolution of the sensor. The RS images (*Fig. 1*) applied in this research were captured on January 3rd,

http://www.aloki.hu ● ISSN 1589 1623 (Print) ● ISSN1785 0037 (Online)
DOI: http://dx.doi.org/10.15666/aeer/2102_15151532

2020 (post deciduous leaf period), September 29th, 2020 (leafy period), November 9th, 2020 (leaves colour changes period) and March 15th, 2021 (flowering and leafing period). The flight height of UAV was ~ 370 m and imaging time was between 12:00 and 13:30 pm. Detailed data acquisition and preprocessing procedures were obtained from a previously reported research (Liu, 2022).

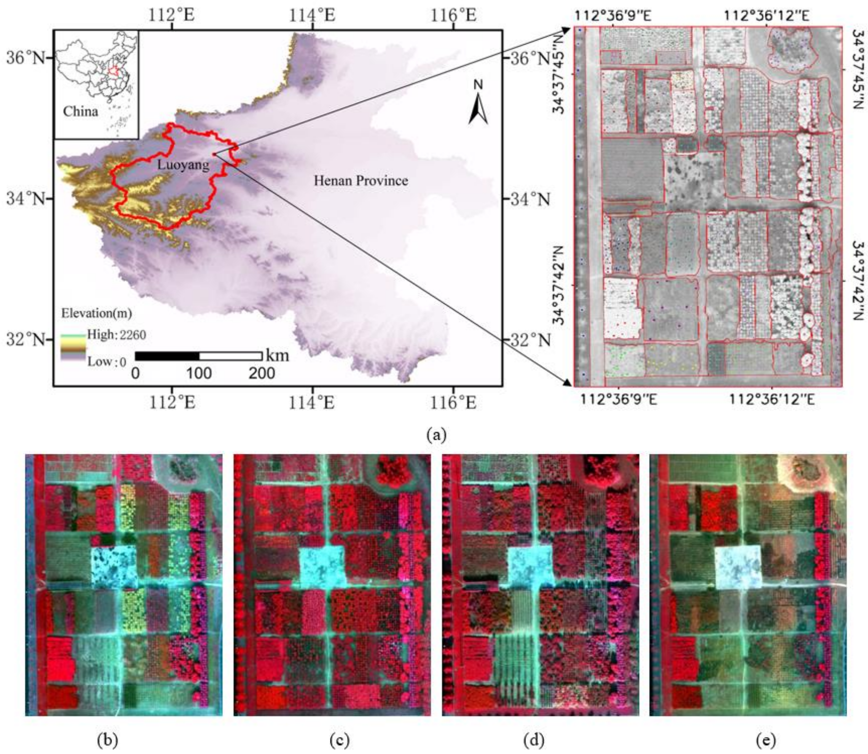

***Figure 1.** Location map of research area and images of test area. (a) Location map of research area; (b) spring image (RGB vs bands 532); (c) summer image; (d) autumn image; (e) winter image*

***Table 1.** Band and spatial resolution parameters of UAV RedEdge-MX multispectral data*

Band number	Band name	Spatial resolution (cm)	Wavelength range (μm)	Central wavelength (μm)
1	Blue	15.00	0.465–0.485	0.475
2	Green		0.550–0.570	0.560
3	Red		0.663–0.673	0.668
4	Red edge		0.712–0.722	0.717
5	Near infrared		0.820–0.860	0.840

Tree species sample data

From April to June 2021, TS information in research area was collected. The TS names belonging to a patch were directly marked, delineated, and recorded on RedEdge-MX standard false colour printed images. The collected outdoor data were applied to train and test urban TS classification. In laboratory, TS sample data were recorded in spreadsheets (*Table 2*) and transformed into Region of Interest (ROI) files, which could be labelled in RedEdge-MX image sets. Detailed TS survey and sample collection procedures were also

http://www.aloki.hu ● ISSN 1589 1623 (Print) ● ISSN1785 0037 (Online)
DOI: http://dx.doi.org/10.15666/aeer/2102_15151532

from a previous study (Liu, 2022). All ROIs (right hand side of *Fig. 1a*) and patches (*Fig. 3a*) of each TS for training and validation samples were delineated on their corresponding images. *Table 2* gives a summary of TS names as well as pixel numbers for training and validation samples.

Table 2. *Scientific names and pixel numbers of training and validation samples for TS classification*

Tree species number	Scientific names	Training samples	Validation samples	Tree species number	Scientific names	Training samples	Validation samples
T1	*Photinia × fraseri*	238	32400	T17	*Paeonia suffruticosa*	237	23733
T2	*Loropetalum chinense* var. *rubrum*	257	11437	T18	*Acer serrulatum*	202	8560
T3	*Platanus orientalis*	238	33840	T19	*Armeniaca mume* f. *rubriflora*	226	34120
T4	*Armeniaca vulgaris*	230	14538	T20	*Acer negundo 'Aurea'*	231	17933
T5	*Punica granatum 'Flavescens'*	274	14476	T21	*Cerasus avium*	207	28549
T6	*Cedrus deodara*	235	20098	T22	*Nandina domestica*	353	17129
T7	*Cinnamomum camphora*	262	24080	T23	*Prunus × blireana 'Meiren'*	230	25496
T8	*Magnolia grandiflora*	206	16593	T24	*Viburnum odoratissimum*	220	3967
T9	*Malus micromalus*	242	33414	T25	*Ligustrum quihoui*	232	7168
T10	*Chaenomeles cathayensis*	263	20711	T26	*Crataegus pinnatifida*	218	7946
T11	*Osmanthus fragrans* var. *semperflorens*	148	13288	T27	*Bischofia polycarpa*	311	27136
T12	*Rosa chinensis*	223	32708	T28	*Koelreuteria paniculata*	255	13973
T13	*Acer palmatum 'Atropurpureum'*	231	13283	T29	*Paeonia lactiflora*	132	5691
T14	*Aesculus chinensis*	238	13582	T30	*Populus tomentosa*	243	14752
T15	*Malus halliana*	247	16280	T31	*Wisteria sinensis*	213	3772
T16	*Michelia champaca*	279	47974	T32	Climbing roses	229	11859

Mask for non-tree parts

After drawing TS patches, grass and bare land patches were drawn and applied vector data to make a mask file to mask out the non-tree parts of the images. In TS classification, the non-tree parts of the images were excluded using the mask file and only the tree parts of the images were retained for TS identification.

Experimental methods

Texture feature extraction

The eight texture feature types, i.e. MEA, VAR, HOM, CON, DIS, ENT, SM and COR, were extracted from 20 bands of four seasons data, and formed eight texture feature sets, each containing 20 texture features. To extract texture features, the co-occurrence measures of ENVI 5.4 were applied and processing window size (first parameter) was considered according to the gradient of 3 × 3, 5 × 5, ..., N × N, and (N + 2) × (N + 2)

http://www.aloki.hu ● ISSN 1589 1623 (Print) ● ISSN1785 0037 (Online)
DOI: http://dx.doi.org/10.15666/aeer/2102_15151532

(where N is texture extraction window size corresponding to the highest accuracy of TS classification and N + 2 is the maximum texture extraction window according to actual requirements). In the second parameter setting, both X and Y values of co-occurrence shift were considered to be 1.

Effectiveness assessment

MLC and RF were respectively applied to determine optimal windows for each texture extraction type. Under these optimal windows, each texture feature type of 20 bands were extracted and applied for TS classification. Then, the effectiveness of various texture features in TS identification was explored according to the accuracy difference of various texture features in TS classification and their classification result maps. In addition, all texture feature types were combined for TS recognition to evaluate the performance of the mixed texture feature set in TS identification. Finally, the mixed texture feature set was combined with 20 spectral bands and 4 DSMs for TS classification and classification results were compared with those of 20 spectral bands, 5 bands of spring data and 4 DSMs. A cross feature type comparison was made to further analyze the performance of texture features in TS classification.

Image classification and result evaluation approaches

Considering the effect of data dimension on the classification performance of classifiers in low-dimensional data sets (e.g., spectral bands and DSMs), both MLC and RF were applied for TS classification. For high-dimensional data sets, only RF was employed for TS classification because MLC was prone to Hughes phenomenon. To do so, ENVI 5.4 (for MLC, all parameters were default) and EnMAP-Box (for RF, all parameters were default) experimental tools used (Van der Linden et al., 2015). After TS identification with all feature sets, validation sample was applied to evaluate all experimental results and generate confusion matrix for accuracy verification. Overall accuracy (OA), Kappa coefficient (KC), producer and user accuracies (producer accuracy is the probability that a pixel in classification image is put into class x given the ground truth class is x and user accuracy is the probability that the ground truth class is x given a pixel is put into class x in the classification image) calculated from the confusion matrix and diagram of curves (generated by OA was used to evaluate the suitability of textures extracted by different processing windows in TS classification), histogram and spider graphs generated by some of them were used to compare and analyse classification results.

Results and analyses

The influence of texture extraction window on TS recognition accuracy

With the increase of the size of texture extraction window, and used the extracted eight types of texture features in different window for tree species classification, the OA changes of 32 kinds of greening TS classification using MLC and RF are shown in *Fig. 2*.

As illustrated in *Fig. 2,* whether using MLC or RF, by increasing texture extraction window, the accuracy of TS classification was first rapidly increased, then gradually stabilized, and finally began to decline. Except for texture feature MEA, in all textures, under the same window, the accuracy of RF classification of TS was higher than that of MLC.

http://www.aloki.hu ● ISSN 1589 1623 (Print) ● ISSN1785 0037 (Online)
DOI: http://dx.doi.org/10.15666/aeer/2102_15151532

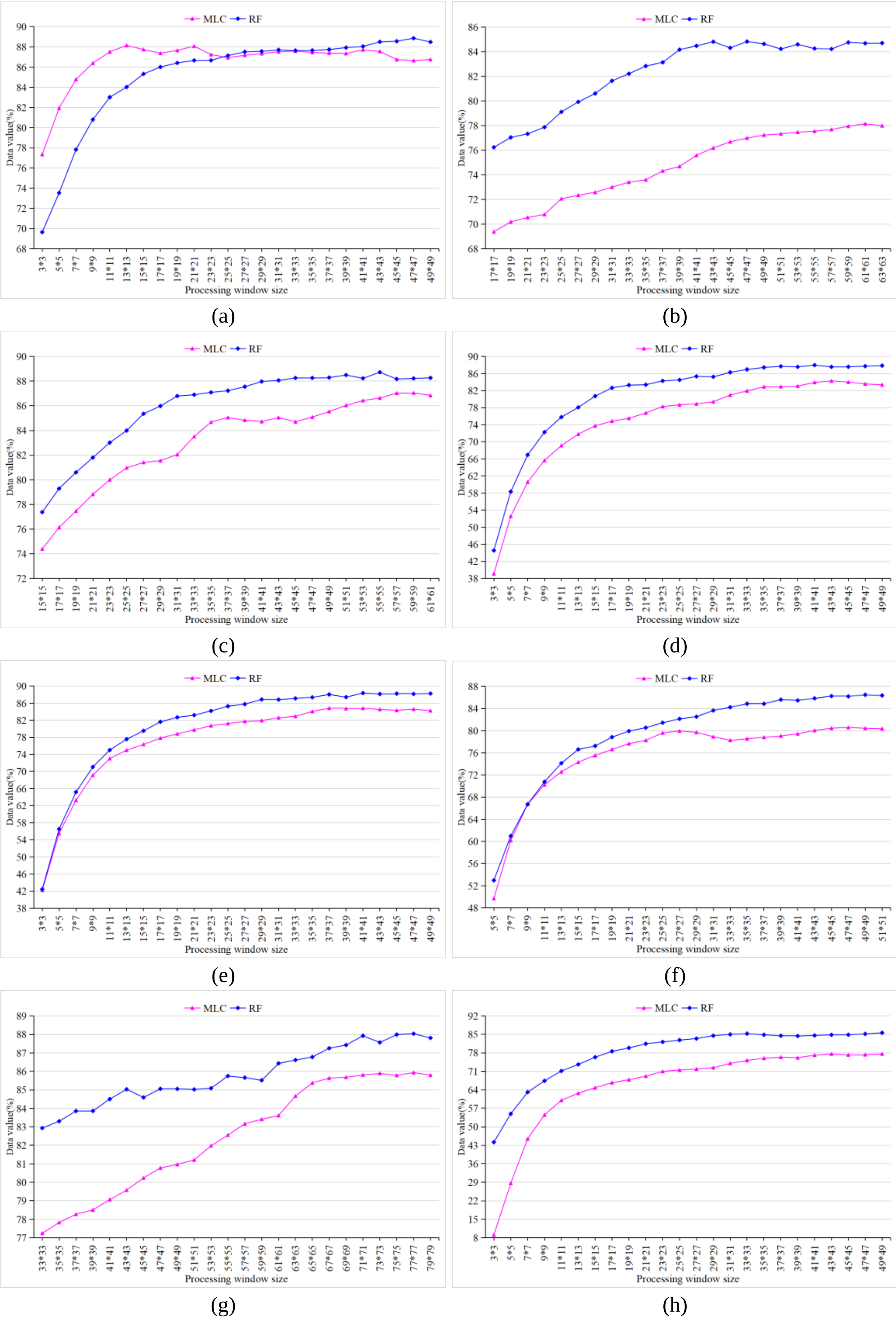

***Figure 2.** The OA change curves of TS classification corresponding to window sizes for texture feature extraction. (a) MEA; (b) VAR; (c) HOM; (d) CON; (e) DIS; (f) ENT; (g) SM; (h) COR*

http://www.aloki.hu ● ISSN 1589 1623 (Print) ● ISSN1785 0037 (Online)
DOI: http://dx.doi.org/10.15666/aeer/2102_15151532

Optimal classification results for each type of texture feature

The optimal extraction windows of various texture features determined by MLC and RF as well as the OA of TS classification obtained under these windows are summarized in *Tables 3* and *4*.

Table 3. *Optimal classification results of each type of texture feature based on MLC*

Texture feature	Optimal extraction window	Overall accuracy%	Kappa coefficient	Order of importance
MEA	13 × 13	88.1440	0.8763	1
VAR	61 × 61	78.1425	0.7721	7
HOM	59 × 59	87.0503	0.8650	2
CON	43 × 43	84.2887	0.8362	5
DIS	37 × 37	84.8083	0.8415	4
ENT	47 × 47	80.5827	0.7975	6
SM	77 × 77	85.9335	0.8533	3
COR	43 × 43	77.5905	0.7667	8

Table 4. *Optimal classification results of each type of texture feature based on RF*

Texture feature	Optimal extraction window	Overall accuracy%	Kappa coefficient	Order of importance
MEA	47 × 47	88.8559	0.8840	1
VAR	47 × 47	84.8180	0.8420	8
HOM	55 × 55	88.7232	0.8826	2
CON	41 × 41	87.9812	0.8749	5
DIS	41 × 41	88.3571	0.8788	3
ENT	49 × 49	86.4724	0.8592	6
SM	77 × 77	88.0387	0.8755	4
COR	33 × 33	85.2803	0.8468	7

As was seen in *Tables 3* and *4*, under the supervision of the same classifier, the optimal extraction windows of various texture features in TS classification were different and some texture features had smaller optimal extraction windows (e.g. MEA) while some other texture features required a larger window for extraction (e.g. SM). Under the supervision of MLC, the OA obtained by various texture features in TS classification greatly varied. For example, the difference between MEA and COR was about 10%. However, under RF supervision, the OA difference of different types of texture features in TS classification was small. For example, the difference of MEA and VAR in TS classification was about 4%. It could be concluded that the importance rankings of the eight texture feature types by the two classifiers were roughly the same.

Advantages and limitations of each texture type

According to the optimal extraction window size required for each texture type in TS classification and the overall accuracy achievable by the two classifiers, the advantages and limitations of each type of texture are given in *Table 5*.

http://www.aloki.hu ● ISSN 1589 1623 (Print) ● ISSN1785 0037 (Online)
DOI: http://dx.doi.org/10.15666/aeer/2102_15151532

Table 5. *Characteristics of each texture type in TS classification*

Texture type	Advantages	Limitations
MEA	Very high classification accuracy	Need for a large texture extraction window for the selection of some classifiers
VAR	–	Need for a large texture extraction window (time-consuming), low classification accuracy
HOM	Very high classification accuracy	Need for a large texture extraction window (time-consuming)
CON	High classification accuracy, moderate level of texture extraction window (saving time)	Great influence of the selection of classifier on classification accuracy
DIS	High classification accuracy, moderate level of texture extraction window (saving time)	Great influence of the selection of classifier on classification accuracy
ENT	–	Need for medium to large texture extraction window and low classification accuracy
SM	Relatively high classification accuracy	Need for very large texture extraction window (time -consuming)
COR	Requiring medium to small texture extraction window (saving time)	Very low classification accuracy

From the perspective of saving time and ensuring classification results in TS classification, appropriate texture features can be selected by referring to the characteristics of various texture features described in *Table 5*.

Classification effect of various texture features

The eight texture feature types were extracted under their optimal texture extraction windows and their best classification results (under RF supervision) for TS identification are shown in *Fig. 3*.

As shown in *Fig. 3*, compared with real TS distribution on the ground, each texture type had a good effect on TS classification and presented a high consistency with actual situations on the ground. However, each texture type had its own shortcomings in the identification of some specific TS.

Quantitative evaluation of the combination of multiple feature types

The combination of each texture feature type extracted under their optimal windows (a mixed texture feature set) was applied for TS classification and the results of combining the mixed texture feature set with spectral bands and DSM for TS classification are summarized in *Table 6*.

As was seen from *Table 6*, when the eight texture feature types were combined for TS classification, OA presented 92.0599% classification accuracy, which was improved compared with single texture feature type (the highest accuracy for this feature type was 88.8559% (*Table 4*)). After combining mixed texture feature set was with spectral bands and DSM, respectively, TS classification accuracy was further improved. When these three feature types were all combined, TS classification accuracy reached the maximum value of 92.7002% (*Table 6*).

http://www.aloki.hu ● ISSN 1589 1623 (Print) ● ISSN1785 0037 (Online)
DOI: http://dx.doi.org/10.15666/aeer/2102_15151532

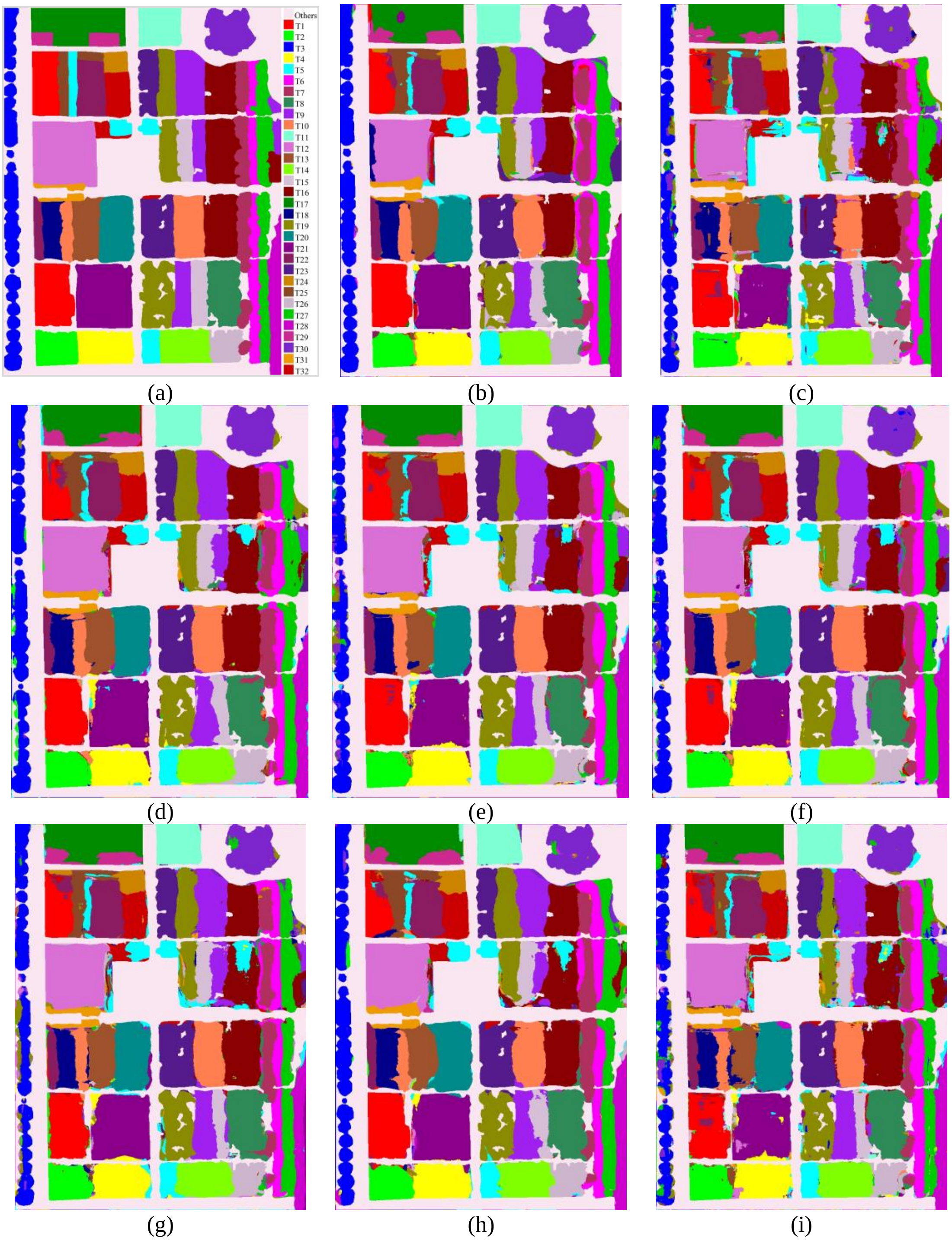

Figure 3. *Results of TS classification using eight texture feature types extracted under their optimal extraction windows. (a) Ground truth; (b) MEA; (c) VAR; (d) HOM; (e) CON; (f) DIS; (g) ENT; (h) SM; (i) COR*

The combination of multi-type features of multi-temporal was applied for TS classification, the accuracy of the obtained classification result was significantly higher than those of single season images (5 bands of spring data, the classification accuracy was the highest in 4 seasons), 20 spectral bands and 4 DSMs of four seasons.

http://www.aloki.hu ● ISSN 1589 1623 (Print) ● ISSN1785 0037 (Online)
DOI: http://dx.doi.org/10.15666/aeer/2102_15151532

***Table 6.** Classification results of TS based on the combination of multi-type features*

Data set	Maximum likelihood classification		Random forest	
	Overall accuracy%	Kappa coefficient	Overall accuracy%	Kappa coefficient
160 textures	–	–	92.0599	0.9173
160 textures + 20 bands	–	–	92.3518	0.9204
160 textures +4 DSMs	–	–	92.3852	0.9207
160 textures + 20 bands+ 4 DSMs	–	–	92.7002	0.9240
20 bands + 4 DSM	77.5088	0.7661	80.4265	0.7965
4 DSMs	67.7565	0.6652	71.1903	0.7007
Four-season 20 bands	72.7582	0.7168	66.4747	0.6522
Spring 5 bands	52.9798	0.5127	50.8216	0.4906

Classification accuracy analysis

The combination of texture features, spectral band and DSM gave the highest OA for TS classification. In the current research, this high-dimensional mixed feature set was the optimal feature set for TS recognition. *Fig. 4* presents the fitted histogram of producer and the user accuracies produced through the optimal feature set for TS classification.

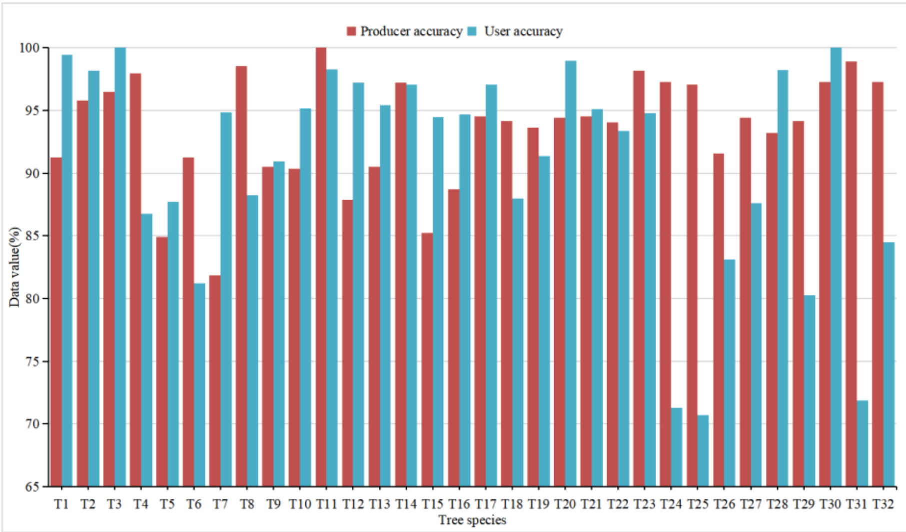

***Figure 4.** Producer and user accuracy histograms of optimal classification results*

Fig. 4 combined with actual data shows that the producer accuracies of 32 greening TS classification using the optimal feature set varied in the range of 81.85% (T7) to 100.00% (T11). Also, the producer accuracies of all TS remained relatively stable (without excessively high or low accuracies). User accuracies ranged from 70.69% (T25) to 100.00% (T3 and T30). Except for the three TS of T24, T25 and T31 (user accuracies of 71.27, 70.69 and 71.84%, respectively), the user accuracies of all other TS remained high. Except for the TS of T24, T25, T29, T31 and T32, the producer and user accuracies of all other TS presented minimal difference. In general, a better result of mapping the 32 greening TS could be achieved by applying the optimal feature set for the classification of target greening TS.

http://www.aloki.hu ● ISSN 1589 1623 (Print) ● ISSN1785 0037 (Online)
DOI: http://dx.doi.org/10.15666/aeer/2102_15151532

Comparison of classification effectiveness of individual TS

Figs. 5a and *b*, respectively, show producer and user accuracy spider web graphs generated using the optimal feature set, 160 texture features, 20 bands, 4 DSMs and spring 5 bands data and their classification maps are illustrated in *Figs. 6a-e*.

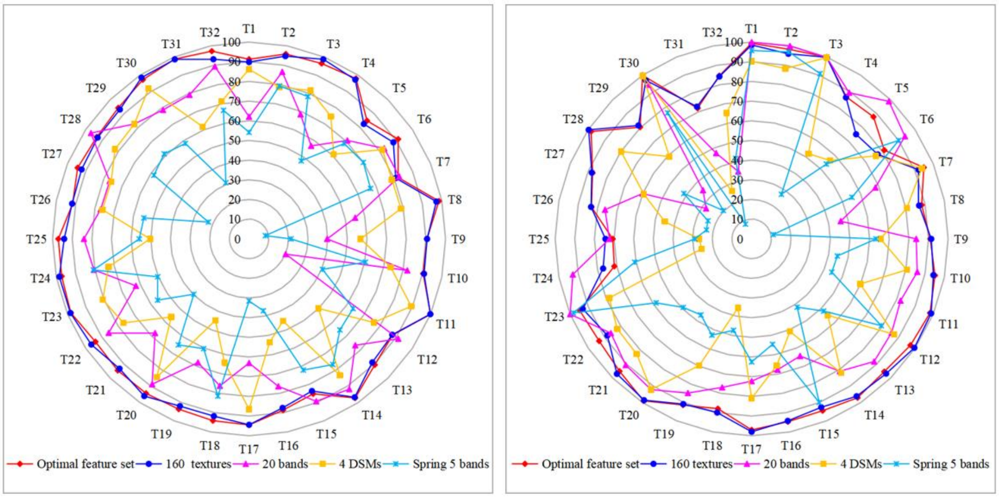

(a) (b)

Figure 5. *Spider web graphs of representative feature set classification results. Spider web graph of (a) producer accuracies and (b) user accuracies*

As illustrated in *Fig. 5*, difference in producer accuracy between the optimal feature set and 160 textures for the classification of 32 greening TS was extremely small. The classification effects of T5, T6, T18, T25, T27 and T32 using the optimal feature set were higher than those obtained using 160 textures while the classification effects of T3, T20 and T22 when using 160 textures were better than those obtained by the optimal feature set. In addition, the producer accuracies of these two data sets for other TS classifications were basically the same.

In terms of user accuracy, the classification effects of T5, T6, T7 and T22 when using the optimal feature set were stronger than those when using 160 textures while the classification effects of T12, T18, T21, T24 and T25 when using 160 textures were better than those obtained by the optimal feature set. Similarly, the user accuracies of the two data sets for the remaining TS classifications were basically the same.

Fig. 5 illustrates that the producer and user accuracy curves of these TS were more convergent to the centre of the circle using 20 bands, 4 DSMs and spring 5 bands data classifications. Furthermore, their classification effects were not as good as the those of the optimal feature set and 160 textures.

From *Figs. 6a* and *b*, it was seen that the mapping results of 32 TS using the optimal feature set and 160 textures were highly consistent with the real situation of ground distribution of TS; however, some TS were erroneously classified as other TS at the edges and inside of the TS patch. For example, in *Fig. 6a*, part of T1 was erroneously classified as T24 and T25, part of T5 was erroneously classified as T25, part of T7 was erroneously classified as T6, and part of T16 was erroneously classified as T23. A similar situation was observed in classification results when 160 textures (*Fig. 6b*) were applied for classifying TS.

http://www.aloki.hu ● ISSN 1589 1623 (Print) ● ISSN1785 0037 (Online)
DOI: http://dx.doi.org/10.15666/aeer/2102_15151532

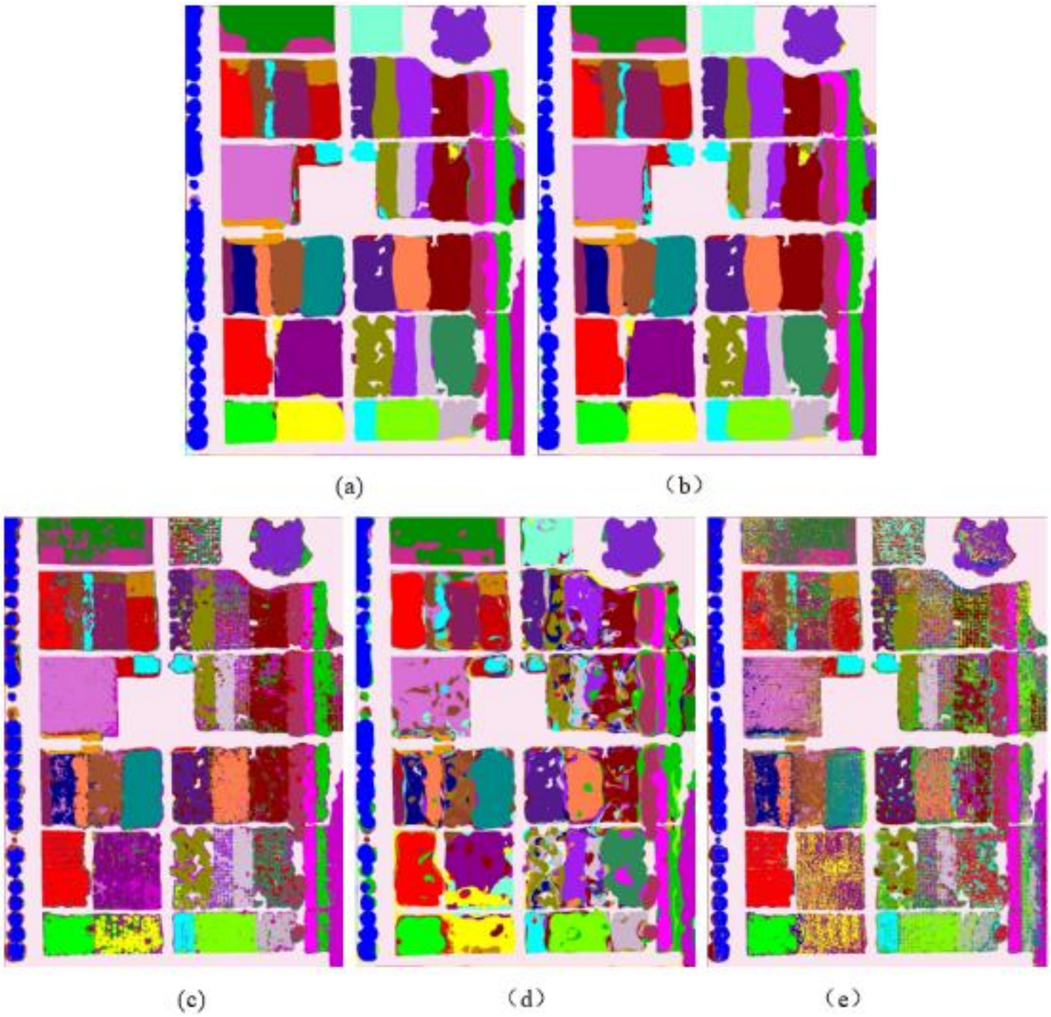

Figure 6. *Comparison of TS classification maps. (a) classification map created with the optimal feature set; (b) classification map created with 160 textures; (c) classification map created with four-season 20 bands; (d) classification map created with 4 DSMs; (e) classification map created with spring 5 bands data*

Using 20 bands, 4 DSMs and spring 5 bands data for classifying TS, certain TS in the classification results presented good recognition effects, but most of the classified TS showed large internal heterogeneities in their distribution patches and recognition effects were weak. Due to the presence of mixed pixels, TS patches created with spring 5 bands data classification had poor homogeneity, whereas those created with 4 DSMs classification presented relatively better homogeneity than the results obtained by 20 bands and spring 5 bands data. The effects of these three data types on TS classification were obviously not as good as those of the best feature set and 160 textures.

Discussion

Eight texture feature types extracted from four seasons RedEdge-MX data played important roles in pure stand TS identification (*Table 4*). Among them, MEA, HOM, DIS and SM had good performance (overall accuracy in the range of 88.0387% to 88.8559%

http://www.aloki.hu ● ISSN 1589 1623 (Print) ● ISSN1785 0037 (Online)
DOI: http://dx.doi.org/10.15666/aeer/2102_15151532

(*Table 4*)). TS classification accuracies using texture features VAR and COR were lower than those of other texture features, but they could also achieve a high accuracy of over 84%. The optimal extraction window sizes of some texture features (such as MEA, HOM, and COR) and their TS recognition accuracy were similar to those reported in the previous study (Liu et al., 2022b). However, there were some differences between these two studies in some texture features (e.g. SM, DIS, and VAR) (Liu et al., 2022b). This difference could be due to the different planting methods of identified TS. In this research, patch pure forest was identified while in the previous study, individual trees were identified. In the follow-up study, based on the summary presented in *Table 5*, the texture features with small optimal extraction windows and high classification accuracies could be selected for pure stand TS recognition.

When the eight texture feature types were fully combined, TS classification accuracy was significantly improved (up to 92.0599% (*Table 6*)), which further proved the importance of these texture feature types in TS identification and also showed that the combination of multiple texture feature types was critical in TS classification. Eight texture feature types were extracted from each band of the four seasons data and the differences of various TS in different bands and time phases were fully evaluated; therefore, the final classification accuracy reached a high level, which could be the main reason why multi-temporal and multi-texture features can drive the identification of pure stand TS. The findings of this research were consistent with previous research conclusions that multi-temporal data had to be applied for TS identification (Li et al., 2015; Pu et al., 2018; Immitzer et al., 2019).

The overall accuracy of the mixed texture feature set constructed by each texture feature type under their own optimal extraction windows for TS classification was 92.0599% (*Table 6*), while that of the mixed texture feature set constructed by the eight texture feature types according to the same optimal extraction windows for TS classification was 91.52% (Liu, 2022). The former was slightly higher than the latter, but there was only a slight difference. A previous study presented the same experimental phenomenon as this study (Liu et al., 2022a). This showed that in TS classification, it was better to extract different texture feature types according to their own optimal windows than the application of the same optimal window, but for convenience, the same window could also be applied for all texture feature extraction types because the two supervision forms showed little difference in overall accuracy.

In this research, when the mixed texture feature set was combined with spectral band and DSM, TS classification accuracy was further improved, but the improvement effect was slight (*Table 6*). However, in previous studies, when multiple feature types were combined, classification accuracy was greatly improved (Liu et al., 2022a,b). The main reason was that this study has obtained the high overall accuracy of TS classification by using the mixed texture feature set, it may be close to the limit of accuracy that the RedEdge-MX dataset can achieve in TS classification, and it becomes very difficult to significantly improve the classification accuracy of TS by combining other useful features. This did not mean that spectral bands and DSM were not important in TS classification. According to the findings of many previous research works (Karlson et al., 2016; Pu et al., 2018; Han et al., 2019; Immitzer et al., 2019), in order to improve TS classification accuracy, it was necessary to combine various types of image features such as spectral band and DSM as much as possible.

RF was more suitable than MLC for the evaluation of the performance of each texture feature type in pure stand TS identification (*Tables 3* and *4*). First, for each texture feature

http://www.aloki.hu ● ISSN 1589 1623 (Print) ● ISSN1785 0037 (Online)
DOI: http://dx.doi.org/10.15666/aeer/2102_15151532

type, TS classification accuracy using RF was higher than that using MLC (*Fig. 2*). Second, the accuracy obtained by RF classification for each type of texture feature was low, while that obtained by MLC was quite different; therefor, RF better reflected whether different feature types played important roles in TS identification. Third, the performance of RF was very robust in high-dimensional dataset classification, while Hughes phenomenon occurred in MLC when these datasets were used, which was not conducive to analyzing whether the high-dimensional texture feature sets could improve the identification effect of TS. A previous study has also confirmed that RF was more suitable than MLC in the evaluation of the importance of different texture features in TS recognition (Liu et al., 2022b).

This study only evaluated the performance of eight texture types in pure forest TS identification in regular plots. In the irregular and non-pure forest environment, the TS recognition performance of the different texture types needs to be further explored in the follow-up study.

Conclusions

In order to investigate the performance of eight texture feature types extracted from UAV RedEdge-MX four-phase images in TS identification of pure stands, this study utilized MLC and RF classifiers to determine the optimal windows for texture extraction and classification of 32 types of greening TS. The following main conclusions were drawn:

(1) Eight texture feature types presented good performance in pure stand TS identification and the texture features MEA and VAR had the best and worst performance, respectively.

(2) The combination of eight texture feature types (mixed texture feature set) further improved the recognition accuracy of TS compared to the application of single-type of texture features.

(3) Although mixed texture feature set achieved high TS recognition accuracy, when it was combined with spectral bands and DSMs, its accuracy was further improved.

(4) TS recognition accuracy using the multi-features of four seasons images was significantly higher than that using single seasonal spectral bands.

This study confirmed that in pure stand TS identification, all eight texture feature types in four seasons had good performance and could be actively recommended for TS identification. It should be noted that when extracting texture features, the optimal extraction window has to be found for each texture feature type and then, a mixed texture feature set has to be constructed because the accuracy obtained by texture feature set for TS recognition is higher than those of all textures extracted using the same optimal window.

Acknowledgments. This work was supported by the National Natural Science Foundation of China (Grant No. 32001250), and the Natural Science Foundation of Henan Province, China (Grant No. 202300410293). I want to provide gratitude to the editors and the anonymous reviewers.

Disclosure statement. No potential conflict of interests was reported by the author.

REFERENCES

[1] Agarwal, A., Kumar, S., Singh, D. (2021): An adaptive technique to detect and remove shadow from drone data. – J. Indian Soc. Remote Sens. 49: 491-498. https://doi.org/10.1007/s12524-020-01227-z.

[2] Åkerblom, M., Raumonen, P., Mäkipää, R., Kaasalainen., M. (2017): Automatic tree species recognition with quantitative structure models. – Remote Sens. Environ. 191: 1-12. https://doi.org/10.1016/j.rse.2016.12.002.

[3] Apostol, B., Petrila, M., Lorenţ, A., Ciceu, A., Gancz, V., Badea, O. (2020): Species discrimination and individual tree detection for predicting main dendrometric characteristics in mixed temperate forests by use of airborne laser scanning and ultra-high-resolution imagery. – Sci. Total Environ. 698: 134074. https://doi.org/10.1016/j.scitotenv.2019.134074.

[4] Cross, M. D., Scambos, T., Pacifici, F., Marshall, W. E. (2019): Determining effective meter-scale image data and spectral vegetation indices for tropical forest tree species differentiation. – IEEE J. Sel. Top. Appl. Earth Obs. Remote Sens. 12(8): 2934-2943. https://doi.org/ 10.1109/JSTARS.2019.2918487.

[5] Dymond, C. C., Mladenof, D. J., Radelof, V. (2002): Phenological differences in tasseled cap indices improve deciduous forest classification. – Remote Sens. Environ. 80(3): 460-472. https://doi.org/10.1016/S0034-4257(01)00324-8.

[6] Ferreira, M. P., Zortea, M., Zanotta, D. C., Shimabukuro, Y. E., de Souza Filho, C. R. (2016): Mapping tree species in tropical seasonal semi-deciduous forests with hyperspectral and multispectral data. – Remote Sens. Environ. 179: 66-78. https://doi.org/10.1016/j.rse.2016.03.021.

[7] Ferreira, M. P., Wagner, F. H., Aragão, L. E. O. C., Shimabukuro, Y. E., de Souza Filho, C. R. (2019): Tree species classification in tropical forests using visible to shortwave infrared WorldView-3 images and texture analysis. – ISPRS J. Photogramm. Remote Sens. 149: 119-131. https://doi.org/10.1016/j.isprsjprs.2019.01.019.

[8] Ghosh, A., Joshi, P. K. (2014): A comparison of selected classification algorithms for mapping bamboo patches in lower gangetic plains using very high-resolution WorldView-2 imagery. – Int. J. Appl. Earth Obs. Geoinf. 26(1): 298-311. https://doi.org/10.1016/j.jag.2013.08.011.

[9] Hamraz, H., Jacobs, N. B., Contreras, M. A., Clark, C. (2019): Deep learning for conifer/deciduous classification of airborne LiDAR 3D point clouds representing individual trees. – ISPRS J. Photogramm. Remote Sens. 158: 219-230. https://doi.org/10.1016/j.isprsjprs.2019.10.011.

[10] Han, W., Zhang, S., Jiao, Q., Wu, H. (2019): Dominant tree species mapping based on multi-temporal CHRIS hyperspectral satellite data. – Forest Inventory and Planning 44(2): 1-6.

[11] Immitzer, M., Atzberger, C., Koukal, T. (2012): Tree species classification with random forest using very high spatial resolution 8-band WorldView-2 satellite data. – Remote Sens. 4(9): 2661-2693. https://doi.org/10.3390/rs4092661.

[12] Immitzer, M., Neuwirth, M., Böck, S., Brenner, H., Vuolo, F., Atzberger, C. (2019): Optimal input features for tree species classification in central europe based on multi-temporal sentinel-2 data. – Remote Sens. 11(22): 2599. https://doi.org/10.3390/rs11222599.

[13] Kamal, M., Phinn, S., Johansen, K. (2015): Object-based approach for multi-scale mangrove composition mapping using multi-resolution image datasets. – Remote Sens. 7(4): 4753-4783. https://doi.org/10.3390/rs70404753.

[14] Karlson, M., Ostwald, M., Reese, H., Bazié, H. R., Tankoano, B. (2016): Assessing the potential of multi-seasonal WorldView-2 imagery for mapping West African agroforestry tree species. – Int. J. Appl. Earth Obs. Geoinf. 50: 80-88. https://doi.org/10.1016/j.jag.2016.03.004.

[15] Kemal, A., Serhat, K., Onur, C. (2019): Classification and diagnosis of cervical cancer with stacked autoencoder and softmax classification. – Expert Syst. Appl. 115: 557-564. https://doi.org/10.1016/j.eswa.2018.08.050.
[16] Kureel, N., Sarup, J., Matin, S., Goswami, S., Kureel, K. (2021): Modelling vegetation health and stress using hyperspectral remote sensing data. – Model. Earth Syst. Environ. https://doi.org/10.1007/s40808-021-01113-8.
[17] Li, D., Ke, Y., Gong, H., Li, X. (2015): Object-based urban tree species classification using bi-temporal WorldView-2 and WorldView-3 images. – Remote Sens. 7(12): 16917-16937. https://doi.org/10.3390/rs71215861.
[18] Lin, C., Popescu, S. C., Thomson, G., Tsogt, K., Chang, C. I. (2015): Classification of tree species in overstorey canopy of subtropical forest using QuickBird images. – Plos One 10(5): e0125554. https://doi.org/10.1371/journal.pone.0125554.
[19] Liu, H. P., An, H. J., Wang, B., Zhang, Q. L. (2015): Tree species classification using WorldView-2 images based on recursive texture feature elimination. – J. Beijing For. Univ. 37(8): 53- 59.
[20] Liu, H., An, H. (2019): Urban greening tree species classification based on HSV colour space of WorldView-2. – J. Indian Soc. Remote Sens. 47(11): 1959-1967. https://doi.org/10.1007/s12524-019-01028-z.
[21] Liu, H., An, H. (2020): Analysis of the importance of five new spectral indices from WorldView-2 in tree species classification. – J. Spatial Sci. 65(3): 455-466.
[22] Liu, H. (2022): Classification of urban tree species using multi-features derived from four-season RedEdge-MX data. – Comput. Electron. Agric. 194: 106794. https://doi.org/10.1016/j.compag.2022.106794.
[23] Liu, H., Su, X., An, H. (2022a): Typical landscape tree species recognition based on RedEdge-MX: suitability analysis of two texture extraction forms under random forest supervision. – Pol. J. Environ. Stud. 31(2): 1475-1484. https://doi.org/10.15244/pjoes/141815.
[24] Liu, H., Su, X., Zhang, C., An, H. (2022b): Landscape tree species recognition using RedEdge-MX: suitability analysis of two different texture extraction forms under MLC and RF supervision. – Open Geosci. 14(1): 985-994. https://doi.org/10.1515/geo-2022-0416.
[25] Masemola, C., Cho, M. A., Ramoelo, A. (2019): Assessing the effect of seasonality on leaf and canopy spectra for the discrimination of an alien tree species, acacia mearnsii, from co-occurring native species using parametric and nonparametric classifiers. – IEEE Trans. Geosci. Remote Sens. 57(8): 5853-5867. https://doi.org/10.1109/TGRS.2019.2902774.
[26] Masemola, C., Cho, M. A., Ramoelo, A. (2020): Sentinel-2 time series based optimal features and time window for mapping invasive australian native acacia species in KwaZulu natal, south Africa. – Int. J. Appl. Earth Obs. Geoinf. 93: 102207. https://doi.org/10.1016/j.jag.2020.102207.
[27] Modzelewska, A., Fassnacht, F. E., Stereńczak, K. (2020): Tree species identification within an extensive forest area with diverse management regimes using airborne hyperspectral data. – Int. J. Appl. Earth Obs. Geoinf. 84: 101960. https://doi.org/10.1016/j.jag.2019.101960.
[28] Naidoo, L., Cho, M. A., Mathieu, R., Asner, G. P. (2012): Classification of savanna tree species, in the Greater Kruger National Park region, by integrating hyperspectral and LiDAR data in a Random Forest data mining environment. – ISPRS J. Photogramm. Remote Sens. 69(3): 167-179. https://doi.org/10.1016/j.isprsjprs.2012.03.005.
[29] Niu, J. N., Sun, Y. M., Zhang, Y. R., Ji, Y. F. (2019): Noise-suppressing channel allocation in dynamic DWDM-QKD networks using LightGBM. – Opt. Express. 27(22): 31741-31756. https://doi.org/10.1364/OE.27.031741.
[30] Pu, R., Landry, S. (2012): A comparative analysis of high resolution IKONOS and WorldView-2 imagery for mapping urban tree species. – Remote Sens. Environ. 124: 516-533. https://doi.org/10.1016/j.rse.2012.06.011.

http://www.aloki.hu ● ISSN 1589 1623 (Print) ● ISSN1785 0037 (Online)
DOI: http://dx.doi.org/10.15666/aeer/2102_15151532

[31] Pu, R., Shawn, L., Yu, Q. (2018): Assessing the potential of multi-seasonal high resolution pléiades satellite imagery for mapping urban tree species. – Int. J. Appl. Earth Obs. Geoinformation 71: 144-158. https://doi.org/10.1016/j.jag.2018.05.005.
[32] Pu, R., Landry, S. (2020): Mapping urban tree species by integrating multi-seasonal high resolution Pléiades satellite imagery with airborne LiDAR data. – Urban For. Urban Gree. 53: 126675. https://doi.org/10.1016/j.ufug.2020.126675.
[33] Richards, J. A., Jia, X. (2008): Using suitable neighbors to augment the training set in hyperspectral maximum likelihood classification. – IEEE Geosci. Remote Sens. Lett. 5(4): 774-777. https://doi.org/10.1109/LGRS.2008.2005512.
[34] Shi, W. W., Gong, Y. H., Tao, X. Y., Cheng, D., Zheng, N. N. (2019): Fine-grained image classification using modified DCNNs trained by cascaded softmax and generalized large-margin losses. – IEEE Trans. Neural Networks Learn. Syst. 30(3): 683-694. https://doi.org/10.1109/TNNLS.2018.2852721.
[35] Shi, Y. F., Wang, T. J., Skidmore, A. K., Heurich, M. (2020): Improving LiDAR-based tree species mapping in Central European mixed forests using multi-temporal digital aerial colour-infrared photographs. – Int. J. Appl. Earth Obs. Geoinf. 84: 101970. https://doi.org/10.1016/j.jag.2019.101970.
[36] Torabzadeh, H., Leiterer, R., Hueni, A., Schaepman, M., Morsdorf, F. (2019): Tree species classification in a temperate mixed forest using a combination of imaging spectroscopy and airborne laser scanning. – Agric. For. Meteorol. 279: 107744. https://doi.org/10.1016/J.AGRFORMET.2019.107744.
[37] Van der Linden, S., Rabe, A., Held, M., Jakimow, B., Leitão, P. J., Okujeni, A., Schwieder, M., Suess, S., Hostert, P. (2015): The EnMAP-Box-A Toolbox and application programming interface for EnMAP data processing. – Remote Sens. 7(9): 11249-11266. https://doi.org/10.3390/rs70911249.
[38] Wang, T., Zhang, H., Lin, H., Fang, C. (2016): Textural-spectral feature-based species classification of mangroves in mai po nature reserve from Worldview-3 imagery. – Remote Sens. 8(1): 24. https://doi.org/10.3390/rs8010024.
[39] Wang, X., Wang, Y., Zhou, C., Yin, L., Feng, X. (2020): Urban forest monitoring based on multiple features at the single tree scale by uav. – Urban For. Urban Gree. 58: 126958. https://doi.org/10.1016/j.ufug.2020.126958.
[40] Yan, S., Jing, L., Wang, H. (2021): A new individual tree species recognition method based on a convolutional neural network and high-spatial resolution remote sensing imagery. – Remote Sens. 13(3): 479. https://doi.org/10.3390/rs13030479.
[41] Yu, X., Hyyppä, J., Litkey, P., Kaartinen, H., Vastaranta, M., Holopainen, M. (2017): Single-sensor solution to tree species classification using multispectral airborne laser scanning. – Remote Sens. 9(2): 108. https://doi.org/10.3390/rs9020108.
[42] Zhang, Z., Kazakova, A., Moskal, L. M., Styers, D. M. (2016): Object-based tree species classification in urban ecosystems using LiDAR and hyperspectral data. – Forests. 7(6): 122. https://doi.org/10.3390/f7060122.
[43] Zhang, H. B., Qiu, D. D., Wu, R. Z., Deng, Y. X., Ji, D. H., Li, T. (2019): Novel framework for image attribute annotation with gene selection XGBoost algorithm and relative attribute model. – Appl. Soft Comput. 80: 57-79. https://doi.org/10.1016/j.asoc.2019.03.017.
[44] Zhang, B., Zhao, L., Zhang, X. (2020): Three-dimensional convolutional neural network model for tree species classification using airborne hyperspectral images. – Remote Sens. Environ. 247: 111938. https://doi.org/10.1016/j.rse.2020.111938.
[45] Zhong, L. H., Hu, L. N., Zhou, H. (2019): Deep learning based multi-temporal crop classification. – Remote Sens. Environ. 221: 430-443. https://doi.org/10.1016/j.rse.2018.11.032.
[46] Zhou, J. H., Zhou, Y. F., Mu, W. S. (2011): Mathematic descriptor for identifying plant species: A case study on urban landscape vegetation. – J. Remote Sens. 15(3): 524-538.